EurJIC
European Journal of Inorganic Chemistry

Full Paper
doi.org/10.1002/ejic.202000780

Chemistry Europe
European Chemical Societies Publishing

Rhodium Pincers

Oxidative Addition of Biphenylene and Chlorobenzene to a Rh(CNC) Complex

Amy E. Kynman,[a] Samantha Lau,[a] Sean O. Dowd,[b] Tobias Krämer,*[b,c] and Adrian B. Chaplin*[a]

Abstract: The synthesis and organometallic chemistry of rhodium(I) complex [Rh(CNC–Me)($SOMe_2$)][BAr^F_4], featuring NHC-based pincer and labile dimethyl sulfoxide ligands, is reported. This complex reacts with biphenylene and chlorobenzene to afford products resulting from selective C–C and C–Cl bond activation, [Rh(CNC–Me)(2,2′-biphenyl)($OSMe_2$)][BAr^F_4] and [Rh(CNC–Me)(Ph)Cl($OSMe_2$)][BAr^F_4], respectively. A detailed DFT-based computational analysis indicates that C–H bond oxidative addition of these substrates is kinetically competitive, but in all cases endergonic: contrasting the large thermodynamic driving force calculated for insertion of the metal into the C–C and C–Cl bonds, respectively. Under equivalent conditions the substrates are not activated by the phosphine-based pincer complex [Rh(PNP-*i*Pr)($SOMe_2$)][BAr^F_4].

Introduction

Combining their strong σ-donor characteristics with the favourable thermal stability and reaction control possible with a *mer*-tridentate geometry, pincer ligands featuring flanking NHC groups have emerged as an attractive ligand class with a diverse variety of applications, particularly in transition metal catalysis.[1,2] The ability of NHCs to form adducts across the periodic table notably allows for rich and varied coordination chemistry. Curiously and despite the enduring prominence of rhodium complexes in organometallic chemistry and catalysis,[3] however, NHC-based pincer complexes of this precious metal have not been widely explored beyond rather innocuous rhodium(I) carbonyl derivatives.[4,5] Guisado-Barrios and Bezuidenhout's mesoionic carbene complex **A**, that promotes selective alkyne homocoupling and hydrothiolation reactions,[6] and Kunz's complexes of homoallyl functionalised CNC ligands, which catalyse the isomerisation of epoxides into ketones in the presence of lithium salts,[7] are notable exceptions and highlight the merit of such endeavour (Scheme 1). As part of our work exploring the chemistry of NHC-based pincer ligands, we have also recently prepared rhodium(I) ethylene complex **C** and shown it to be a highly effective catalyst for terminal alkyne homocoupling reactions and, in the case of aryl-substituted substrates, the subsequent formation of bicyclo[4.2.0]octa-1,5,7-trienes.[8,9]

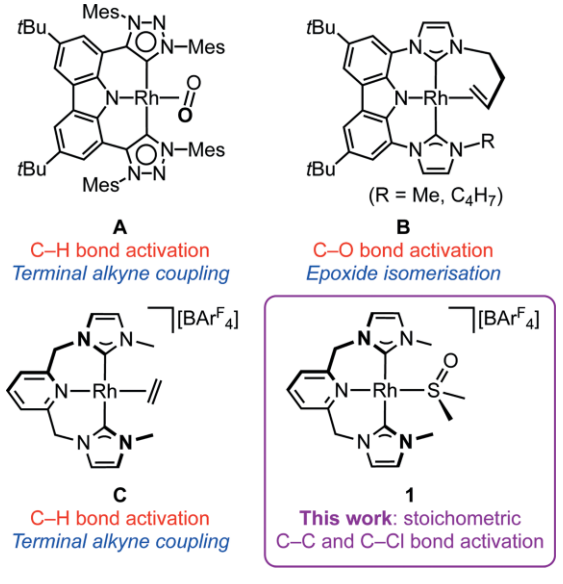

Scheme 1. Reactivity and catalytic activity of selected Rh(CNC) pincer complexes.

In the context of advancing the organometallic chemistry of rhodium complexes of NHC-based pincer ligands relevant to

[a] A. E. Kynman, Dr. S. Lau, Dr. A. B. Chaplin
Department of Chemistry, University of Warwick,
Gibbet Hill Road, Coventry CV4 7AL, UK
E-mail: a.b.chaplin@warwick.ac.uk
http://go.warwick.ac.uk/abchaplin
[b] S. O. Dowd, Dr. T. Krämer
Department of Chemistry, Maynooth University,
Co. Kildare, Maynooth, Ireland.
E-mail: tobias.kraemer@mu.ie
http://www.maynoothuniversity.ie/people/tobias-kr-mer
[c] Dr. T. Krämer
Hamilton Institute, Maynooth University,
Co. Kildare, Maynooth, Ireland
Supporting information and ORCID(s) from the author(s) for this article are available on the WWW under https://doi.org/10.1002/ejic.202000780.

This manuscript is part of the Special Collection Pincer Chemistry and Catalysis.

Full Paper
doi.org/10.1002/ejic.202000780

catalysis, we herein report the capacity of dimethyl sulfoxide complex **1** to undergo the selective oxidative addition of the C–C bond of biphenylene, and C–Cl bond of chlorobenzene. There is precedent for reactivity of this type for rhodium,[10,11] but examples involving pincer ligands are limited to the activation of aryl chlorides by neutral systems.[12] DFT calculations have been used to gain molecular insight and the reactivity of **1** is contrasted to that of [Rh(PNP-*i*Pr)(SOMe$_2$)][BAr$^F_4$] (**2**, PNP-*i*Pr = 2,6-(*i*Pr$_2$PCH$_2$)$_2$C$_5$H$_3$N), containing a less strongly donating but more commonly employed phosphine-based pincer ligand.[13,14]

Results and discussion

1. Convenient new synthesis of 1

We have previously reported that **1** can by isolated following reaction of **C** with dimethyl sulfoxide, however, the preparation of **C** is a rather involved three-step procedure from the proligand CNC–Me•2HBr, the intermediates involved are appreciably air-sensitive, and **1** was only obtained with an overall yield of 26%.[8] As a more accessible method for this latent source of the reactive {Rh(CNC–Me)}$^+$ fragment, we have therefore developed the procedure depicted in Scheme 2. This procedure involves *in situ* generation of the silver(I) carbene transfer agent [Ag(CNC–Me)]$_2$[BAr$^F_4$]$_2$,[15] and subsequent transmetallation with Milstein's underexploited rhodium(I) precursor [RhCl(SOMe$_2$)$_3$] in dichloromethane.[16] In this way pristine **1** was obtained in 50% isolated yield, following straightforward crystallisation from dichloromethane/hexane at RT The spectroscopic characteristics of **1** obtained in this manner are fully congruent with those previously reported, with the *N*–Me (δ_{1H} 3.83) and diastereotopic *N*-CH$_2$ (δ_{1H} 4.95, 5.87) proton resonances the most diagnostic in CD$_2$Cl$_2$.[8]

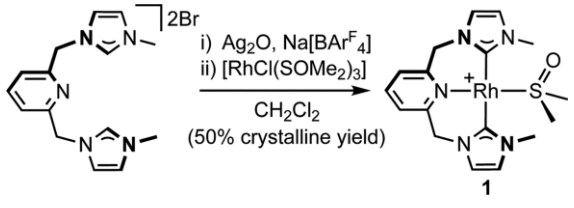

Scheme 2. Convenient synthesis of **1** ([BAr$^F_4$]$^-$ counter anion omitted).

2. Reaction of 1 with biphenylene

In the weakly coordinating solvent 1,2-difluorobenzene (DFB),[17] **1** reacts readily with biphenylene (2 equiv.) at RT to afford the rhodium(III) complex [Rh(CNC–Me)(2,2′-biphenyl)(OSMe$_2$)][BAr$^F_4$] **3**, with 74% conversion observed after 24 h (Figure 1). No intermediates were observed *in situ* by ^{1}H NMR spectroscopy during the reaction and when this reaction was repeated at 50 °C, **3** was obtained in quantitative spectroscopic yield within 3 h. The new complex was subsequently isolated in 74% yield on a larger scale under similar conditions and fully characterised, including in the solid state by single-crystal X-ray diffraction. The formation of **3** is marked in solution by an upfield shift of the *N*–Me (δ_{1H} 2.68 cf. 3.83) and enhanced separation of the diastereotopic *N*-CH$_2$ (δ_{1H} 5.01, 6.02 *cf.* 4.95, 5.87) proton resonances, but overall C_2 symmetry indicates dynamic dissociation of dimethyl sulfoxide (δ_{1H} 2.26 *cf.* free 2.55) and fast pseudo rotation of the 2,2′-biphenyl ligand on the NMR timescale.[5b,18] In the solid state the sulfoxide is bound through the oxygen atom (2.307(2) Å) and this change in coordination mode compared to **1** is in line with expectation for the increase in metal oxidation state. The structure is also notable for an appreciable disparity in the Rh–C contacts associated with the 2,2′-biphenyl ligand (2.013(4), 1.997(4) Å), with the shorter bond *trans* to weakly bound sulfoxide in accord with *trans*-influence arguments: in a closely related macrocyclic analogue, where the coordination sphere is completed instead by an agostic interaction, the difference in Rh–C contacts is more pronounced (2.021(2), 1.992(3) Å).[5c]

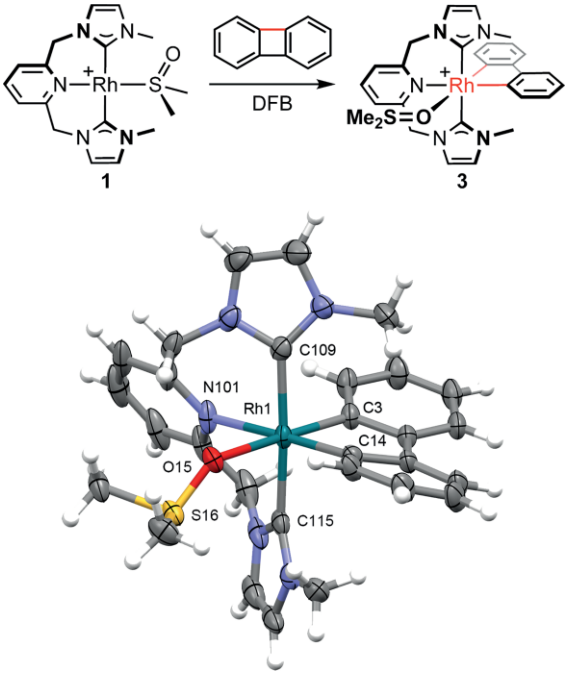

Figure 1. Activation of biphenylene, [BAr$^F_4$]$^-$ counter anions omitted (top). Solid-state structure of **3**, with thermal ellipsoids drawn at 30% probability and solvent omitted (bottom). Selected bond lengths [Å] and angles [deg]: Rh1–N101, 2.239(3); Rh1–C109, 2.051(4); Rh1–C115, 2.077(4); Rh1–C3, 2.013(4); Rh1–C14, 1.997(4); Rh1–O15, 2.307(2); C109–Rh1–C115, 173.99(16); C3–Rh1–C14, 80.34(15); N101–Rh1–C14, 177.40(15); O15–Rh1–C3, 174.94(12).

The formation of **3** is faster than activation of biphenylene by [Rh(P*i*Pr$_3$)$_2$(C$_6$H$_5$F)][BAr$^F_4$] (5 days @ 40 °C), which proceeds under similar conditions via an intermediate η^6-biphenylene derivative and results in the formation of [Rh(P*i*Pr$_3$)$_2$(2,2′-biphenyl)][BAr$^F_4$].[10a] Calculations support a mechanism involving ring slippage and concerted C–C bond oxidative addition in this case. Insertion of the metal into the C–C bond of biphenylene has been reported for iridium pincer complexes {Ir(PCP)} (PCP = 2,6-(*t*Bu$_2$PCH$_2$)$_2$C$_6$H$_3$, 2,6-(*i*Pr$_2$PCH$_2$)$_2$C$_6$H$_3$) and these more structurally similar systems are a valuable mechanistic reference point.[19] Formation of the 2,2′-biphenyl product is complete within 30 min at RT for the less bulky *i*Pr-substituted variant, but thermolysis at 125 °C for 24 h is required for the *t*Bu-substi-

Full Paper
doi.org/10.1002/ejic.202000780

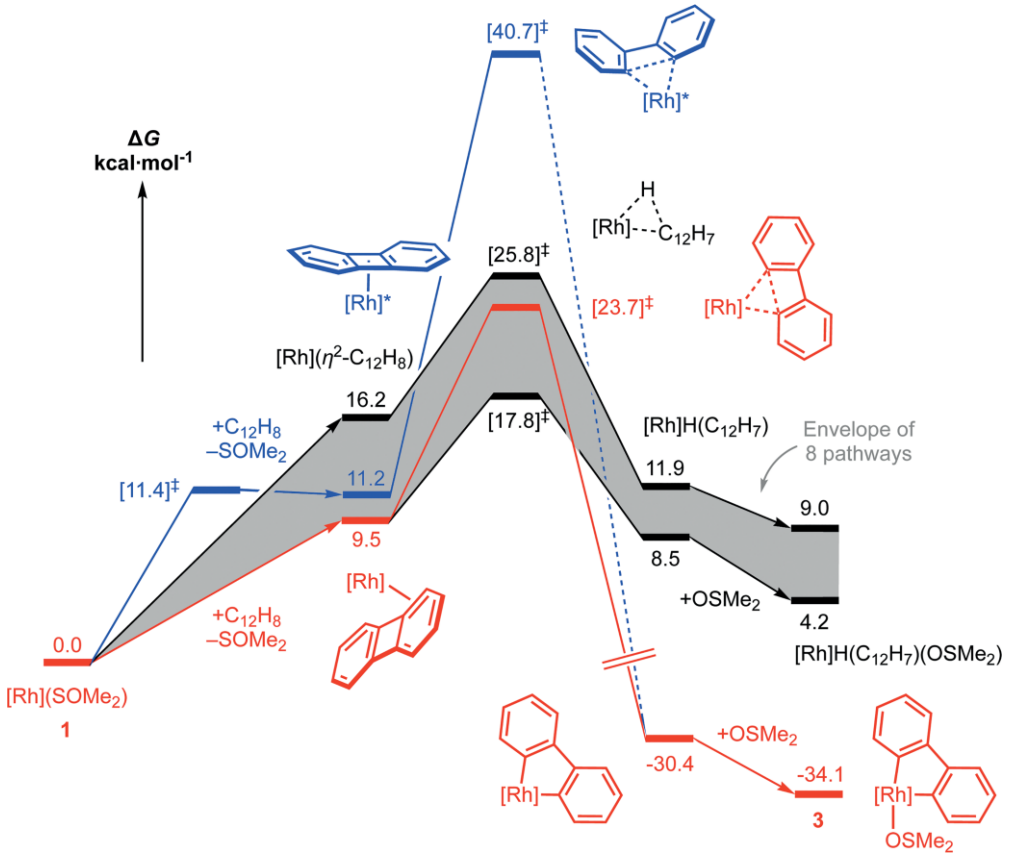

Figure 2. Calculated reaction profiles for the C–H (black, envelope of 8 pathways shown) and C–C (blue and red) bond activation of biphenylene. Arrows depict substitution and association reactions; dashed line represents multiple elementary steps. [Rh] = [Rh(*mer*-CNC–Me)]$^+$, [Rh]* = [Rh(*fac*-CNC–Me)]$^+$.

tuted variant. The attenuated nature of the latter usefully, however, enabled kinetic products of biphenylene C–H bond activation (6-position) to be isolated. As we have previously demonstrated the CNC–Me pincer ligand is able to interconvert between *mer*- and *fac*-coordination modes,[9] both aforementioned mechanistic scenarios – π complex formation and intermediate C–H bond activation – are possible and we turned to DFT calculations using the M06-L/SDD/6-31G(d,p) level of theory to help quantify the viability of these possibilities (Figure 2).

Ring flipping of one of the bridging methylene groups of the pincer backbone ($\Delta G^{‡}$ = 11.4 kcal mol^{-1}), is predicted to enable coordination of biphenylene through the central cyclobutadiene ring, *viz.*, [Rh(*fac*-CNC–Me)(η^4-biphenylene)]$^+$, upon substitution of dimethyl sulfoxide and is associated with a small energetic penalty of ΔG = +11.2 kcal mol^{-1}. Subsequent C–C bond insertion, however, gives rise to a prohibitively high calculated barrier ($\Delta G^{‡}$ = 40.7 kcal mol^{-1} from **1**) ruling out this mechanism. Eight distinct pathways were identified for the C–H bond activation of biphenylene, with calculated activation barriers ranging from $\Delta G^{‡}$ = 17.8 to 25.8 kcal mol^{-1}, but all give rise to thermodynamically unfavourable rhodium(III) products (ΔG = +4.2–9.0 kcal mol^{-1}). Whilst C–C bond oxidative addition is associated with a generally higher calculated barrier ($\Delta G^{‡}$ = 23.7 kcal mol^{-1} from **1**), the reaction proceeds downhill by ΔG = –34.1 kcal mol^{-1} in line with expectation for the associated relief of ring strain.[20] The computational analysis thus suggests: (a) the pincer ligand maintains a *mer*-coordination mode throughout the reaction, (b) whilst faster, competing C–H bond is reversible, and (c) formation of **3** is the only thermodynamically favoured product and is irreversible. These conclusions are fully consistent with experiment; notably the lack of intermediates observed experimentally during the formation of **3**.

In contrast to the activation observed for **1**, no reaction was apparent upon heating **2** with biphenylene (2 equiv.) in DFB at 50 °C for 24 h.

3. Reaction of 1 with Chlorobenzene

On turning to the reaction between **1** and chlorobenzene, it quickly became apparent from *in situ* NMR experiments that more forcing conditions were required to induce reactivity compared to the oxidative addition of biphenylene. Using 100 equivalents of substrate, 15% conversion into [Rh(CNC–Me)(Ph)Cl(OSMe$_2$)][BAr$^F_4$] **4** was observed at RT after 24 h (Figure 3). Higher conversion could be achieved at 50 °C (62% after 24 h), with **4** obtained in quantitative spectroscopic yield within 6 h when the reaction was repeated at 85 °C. This new rhodium(III) complex was subsequently prepared on a larger scale and fully characterised, including in the solid state by single-crystal X-ray diffraction. Complex **4** is characterised in CD_2Cl_2 solution by sharp ^{1}H and ^{13}C resonances that indicate adoption of C_1 symmetry (*N*–Me,

Full Paper
doi.org/10.1002/ejic.202000780

δ_{1H} 3.32, 4.39; *N*-CH_2, δ_{1H} 4.13, 4.57, 5.11, 6.44; Rh–C(Ph), δ_{13C} 142.7, $^1J_{RhC}$ = 32 Hz). Coordination of dimethyl sulfoxide is presumed to be dynamic on the NMR time scale by comparison to **3** and the magnitude of the ^{1}H chemical shift (δ_{1H} 2.51 *cf.* free 2.55). On the basis of the solid-state structure and supported by a computational analysis of the possible isomers, we assign a square pyramidal structure in solution with the free coordination site *trans* to the aryl. A conclusion congruent with the considerably larger *trans*-influence of the aryl compared that of the halide. Indeed, this difference can be quantified directly by comparison of the solid-state metrics of **3** and **4**, where a considerably shorter Rh–N contact is evident for the latter (2.091(3) *cf.* 2.239(3) Å) despite the other common metal-based being very similar (e.g. Rh1–C3 = 2.013(4) Å, **3**; 2.006(4) Å, **4**).

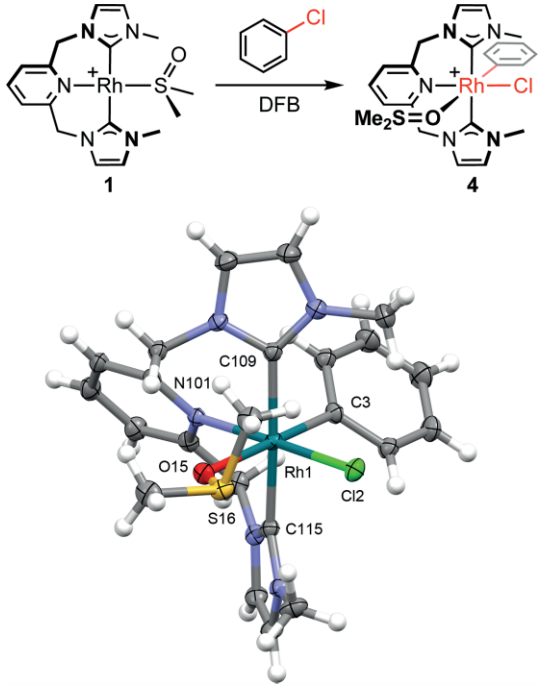

Figure 3. Activation of chlorobenzene, $[BAr^F_4]^-$ counter anions omitted (top). Solid-state structure of **4**, with thermal ellipsoids drawn at 30% probability and solvent omitted (bottom). Selected bond lengths [Å] and angles [deg]: Rh1–N101, 2.091(3); Rh1–C109, 2.053(4); Rh1–C115, 2.063(4); Rh1–C3, 2.006(4); Rh1–Cl2, 2.3584(10); Rh1–O15, 2.310(3); C109–Rh1–C115, 175.12(16); C3–Rh1–Cl2, 91.44(12); N101–Rh1–Cl2, 176.57(9); O15–Rh1–C3, 179.20(14).

Computational analysis of the activation of chlorobenzene by **1** yields a similar picture to that found for biphenylene (Figure 4). In this case, the ability of the pincer ligand to adopt a *fac*-coordination mode enables a sequence involving η^4-coordination of the substrate, ring slippage, and oxidative addition of the C–Cl bond to be more competitive with "direct" insertion ($\Delta\Delta G^‡$ = +2.4 kcal mol^{-1} from **1**) than the biphenylene equivalent ($\Delta\Delta G^‡$ = +17.0 kcal mol^{-1} from **1**).[21] The "direct" insertion pathway proceeds via formation of a κ_{Cl}-adduct of chlorobenzene and is associated with an overall calculated barrier of $\Delta G^‡$ = +26.1 kcal mol^{-1}, which is higher than that predicted for the C–C bond activation of biphenylene ($\Delta G^‡$ = +23.7 kcal mol^{-1}) but in line with the relative reactivity observed experimentally. Ten distinct pathways were identified for the C–H bond activation of chlorobenzene. Some of these compete kinetically with the thermodynamically preferred insertion of the metal into the C–Cl bond (ΔG = –22.3 kcal mol^{-1}), but all are distinctly endergonic. Computational analysis of the activation of chlorobenzene by a related neutral Rh(PNP) pincer come to a similar conclusion.[22]

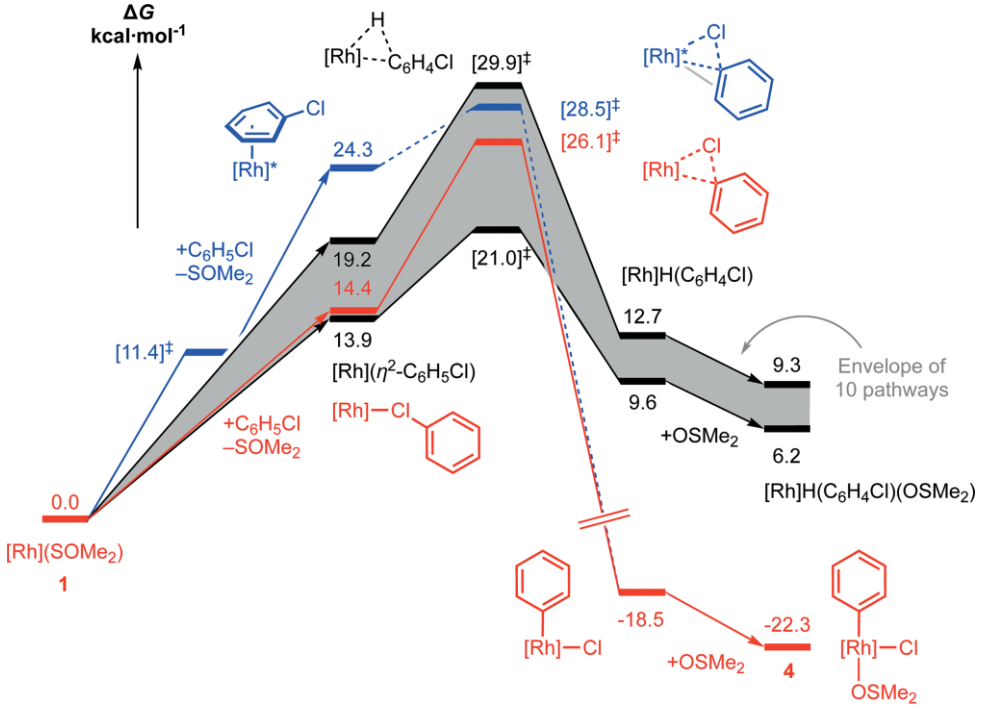

Figure 4. Calculated reaction profiles for the C–H (black, envelope of 10 pathways shown) and C–Cl (blue and red) bond activation of chlorobenzene. Arrows depict substitution and association reactions; dashed line represents multiple elementary steps. [Rh] = [Rh(*mer*-CNC–Me)]$^+$, [Rh]* = [Rh(*fac*-CNC–Me)]$^+$.

Full Paper
doi.org/10.1002/ejic.202000780

In contrast to the activation observed for **1**, no reaction was apparent upon heating **2** with chlorobenzene (100 equiv.) in DFB at 85 °C for 24 h.

Conclusions

We have shown that [Rh(CNC–Me)($SOMe_2$)][BAr^F_4] is a readily accessible rhodium(I) complex of a NHC-based pincer ligand, which undergoes the selective oxidative addition of the C–C bond of biphenylene and the C–Cl bond of chlorobenzene. A detailed DFT-based computational analysis indicates that C–H bond activation of these substrates is kinetically competitive, but in all cases endergonic: contrasting the large thermodynamic driving force calculated for insertion of the metal into the C–C and C–Cl bonds, respectively. The decisive role of the flanking NHC donor groups was confirmed by comparison to a phosphine-based analogue [Rh(PNP-*i*Pr)($SOMe_2$)][BAr^F_4], for which activation of biphenylene and chlorobenzene was not observed under the same conditions. The reactivity characteristics of [Rh(CNC–Me)($SOMe_2$)][BAr^F_4] are of interest from the point of view of homogeneous catalysis and we hope these findings will stimulate greater exploitation of Rh(CNC) complexes in organic synthesis.

Experimental Section

1. General Methods

All manipulations were performed under an atmosphere of argon using Schlenk and glove box techniques unless otherwise stated. Glassware was oven dried at 150 °C overnight and flame-dried under vacuum prior to use. Molecular sieves were activated by heating at 300 °C in vacuo overnight. CD_2Cl_2 was freeze-pump-thaw degassed and dried with 3 Å molecular sieves. 1,2-Difluorobenzene (DFB) and fluorobenzene were pre-dried with alumina, distilled from CaH_2 and dried twice over 3 Å molecular sieves. CD_2Cl_2 and chlorobenzene were dried with 3 Å molecular sieves and stored under an argon atmosphere. All other anhydrous solvents were purchased from Sigma Aldrich or Acros and stored over 3 Å molecular sieves. CNC-Me•2HBr,[23] Na[BAr^F_4],[24] [$RhCl(SOMe_2)_3$],[16] [$Rh(COD)_2$][BAr^F_4][25] and PNP-*i*Pr[26] were prepared following literature procedures. All other reagents are commercially available and were used as supplied. NMR spectra were recorded using Bruker spectrometers under argon at 298 K unless otherwise stated. Chemical shifts are quoted in ppm and coupling constants in Hz. NMR spectra in DFB were recorded using an internal capillary of C_6D_6.[17] HR ESI-MS were recorded on a Bruker MaXis mass spectrometer and microanalyses performed at the London Metropolitan University by Stephen Boyer.

2. Preparation of [Rh(CNC-Me)($SOMe_2$)][BAr^F_4] (1)

A suspension of CNC-Me•2HBr (100 mg, 0.293 mmol), Na[BAr^F_4] (284 mg, 0.320 mmol), and Ag_2O (70.0 mg, 0.303 mmol) in CH_2Cl_2 (5 mL) was stirred in the absence of light for 18 h. The solution was filtered through a Celite plug and added dropwise to a stirred solution of [$RhCl(SOMe_2)_3$] (92.2 mg, 0.293 mmol) in CH_2Cl_2 (2 mL). The resulting suspension was stirred in the absence of light for 2 h, filtered and then layered with hexane to afford the product as red crystals on diffusion at RT. Yield: 192 mg (50%). This complex is unstable in the solid-state outside of an inert atmosphere: complete decomposition observed after 24 h. Spectroscopic data are consistent with the literature.[8]

^{1}H NMR (300 MHz, CD_2Cl_2): δ 7.69–7.75 (m, 8H, Ar^F), 7.68 (t, $^3J_{HH}$ = 7.9, 1H, py), 7.55 (br, 4H, Ar^F) 7.32 (d, $^3J_{HH}$ = 7.8, 2H, py), 7.07 (br, 2H, NCH), 6.80 (br, 2H, NCH), 5.87 (vbr, 2H, CH_2) 4.95 (vbr, 2H, CH_2) 3.83 (s, 6H, NCH_3) 3.15 (s, 6H, $SOMe_2$).

3. NMR scale reactions of [Rh(CNC-Me)($SOMe_2$)][BAr^F_4] (1)

Reactions were performed using 20 mmolL^{-1} solutions of **1** in DFB within J. Young valve NMR tubes and monitored periodically by ^{1}H NMR spectroscopy.

4. Synthesis of [Rh(PNP-*i*Pr)($SOMe_2$)][BAr^F_4] (2)

This complex was prepared by successive substitution of cyclooctadiene from [$Rh(COD)_2$][BAr^F_4] by the pincer ligand (Scheme 3), and thereafter $SOMe_2$ using a methodology developed in our laborotories.[14]

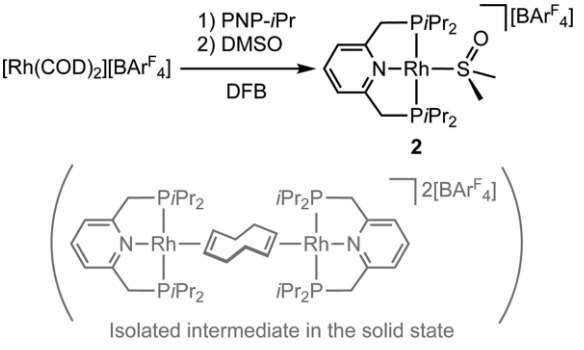

Scheme 3. Preparation of **2** and isolated [{Rh(PNP-*i*Pr)}$_2$(μ_2-η^2:η^2-COD)][BAr^F_4]$_2$ intermediate.

4.1. Preparation of [{Rh(PNP-*i*Pr)}$_2$(μ_2-η^2:η^2-COD)][BAr^F_4]$_2$

A solution of [$Rh(COD)_2$][BAr^F_4] (302 mg, 0.26 mmol) and PNP-*i*Pr (87.7 mg, 0.26 mmol) in DFB (3 mL) was stirred at RT for 12 to give an orange solution. The solution was layered with hexane to yield an orange crystalline solid, which was characterised in the solid state by X-ray diffraction and combustion analysis. Yield: 316 mg (45%). This structure of this compound is less well-defined in solution as a result of dynamic fragmentation.

^{31}P{^{1}H} NMR (121 MHz, DFB/C_6D_6): δ = 44.4 (d, $^1J_{RhP}$ = 134).

Anal. Calcd for $C_{110}H_{106}B_2F_{48}N_2P_4Rh_2$ (2719.32 g mol^{-1}): C, 48.59; H, 3.93; N, 1.03; found C, 48.46; H, 4.04; N, 1.03.

4.2. Preparation of [Rh(PNP-*i*Pr)($SOMe_2$)][BAr^F_4] (2)

A solution of [{Rh(PNP-*i*Pr)}$_2$(μ_2-η^2:η^2-COD)][BAr^F_4]$_2$ (19.8 mg, 7.3 μmol) and $SOMe_2$ (0.10 mL) in DFB (2 mL) was stirred at RT for 12 h. The solution was layered with hexane (*ca.* 20 mL) to afford the product as a yellow crystalline solid on diffusion. Yield: 15.0 mg (74%).

^{1}H NMR (500 MHz, CD_2Cl_2): δ 7.73 (t, $^3J_{HH}$ = 7.8, 1H, py), 7.74–7.69 (m, 8H, Ar^F), 7.56 (br, 4H, Ar^F), 7.36 (d, $^3J_{HH}$ = 7.8, 2H, py), 3.41 (vt, J_{PH} = 4, 4H, CH_2), 3.26 (s, 6H, $SOMe_2$), 2.24–2.39 (m, 4H, 2 × CH), 1.34 (app q, J = 8, 12H, CH_3), 1.09 (app q, J = 7, 12H, CH_3).

^{13}C{^{1}H} NMR (126 MHz, CD_2Cl_2): δ 163.8 (vt, J_{PC} = 6, py), 162.1 (q, $^1J_{CB}$ = 50, Ar^F), 139.5 (s, py), 135.2 (s, Ar^F), 129.3 (qq, $^2J_{FC}$ = 32, $^3J_{CB}$ = 3, Ar^F), 125.0 (q, $^1J_{FC}$ = 272, Ar^F) 121.8 (vt, J_{PC} = 5, py), 117.9 (sept, $^3J_{FC}$ = 4, Ar^F), 53.9 (s, $SOMe_2$), 35.3 (vt, J_{PC} = 10, CH_2), 25.5 (vtd, J_{PC} = 12, $^2J_{RhC}$ = 1, CH), 19.7 (vt, J_{PC} = 3, CH_3), 18.3 (s, CH_3).

$^{31}P\{^1H\}$ NMR (121 MHz, CD_2Cl_2): δ = 55.4 (d, $^1J_{RhP}$ = 137).

Anal. Calcd for $C_{53}H_{53}BF_{24}NOP_2RhS$ (1383.67 g mol^{-1}): C, 46.01; H, 3.86; N, 1.01; found C, 46.18; H, 3.71; N, 1.01.

HR ESI-MS (180 °C, 4 kV) positive ion: 520.1413 ([*M*]$^+$, calcd. 520.1434) *m/z*.

5. NMR scale reactions of [Rh(PNP-*i*Pr)(SOMe$_2$)][BAr$^F_4$] (2)

Reactions were performed using 20 mmolL^{-1} solutions of **2** in DFB within J. Young valve NMR tubes and monitored periodically by ^1H and ^{31}P NMR spectroscopy.

6. Preparation of [Rh(CNC-Me)(2,2′-biphenyl)(OSMe$_2$)][BAr$^F_4$] (3)

A solution of **1** (26.2 mg, 20.0 μmol) and biphenylene (3.04 mg, 20.0 μmol) in DFB (0.5 mL) was heated at 50 °C for 16 h. The resulting solution was layered with hexane to afford the yellow crystalline product on diffusion. Yield: 23 mg (78%).

^1H NMR (500 MHz, CD_2Cl_2): δ 8.04 (t, $^3J_{HH}$ = 7.7, 1H, py), 7.69–7.76 (m, 8H, Ar^F), 7.64 (d, $^3J_{HH}$ = 7.7, 2H, py), 7.56 (br, 4H, Ar^F), 7.36 (d, $^3J_{HH}$ = 7.5, 2H, biph), 7.03 (br, 2H, biph), 6.99 (br, 2H, NCH), 6.97 (d, $^3J_{HH}$ = 7.6, 2H, biph), 6.73 (t, $^3J_{HH}$ = 7.5, 2H, biph), 6.64 (br, 2H, NCH), 6.02 (vbr, 2H, CH_2), 5.01 (vbr, 2H, CH_2), 2.68 (s, 6H, NCH_3), 2.26 (s, 6H, $SOMe_2$).

$^{13}C\{^1H\}$ NMR (126 MHz, CD_2Cl_2): δ 175.6 (d, $^1J_{RhC}$ = 43, NCN), 163.2 (HBMC, biph), 162.3 (q, $^1J_{CB}$ = 50, Ar^F), 156.7 (s, py), 154.3 (s, biph), 140.6 (s, py), 135.3 (s, Ar^F), 135.1 (s, biph), 129.4 (qq, $^2J_{FC}$ = 32, $^3J_{CB}$ = 3, Ar^F), 125.8 (s, py), 125.2 (q, $^1J_{FC}$ = 272, Ar^F), 125.0 (s, biph), 124.2 (s, NCH), 123.2 (s, biph), 121.6 (s, NCH), 120.5 (s, biph), 118.0 (sept, $^3J_{FC}$ = 4, Ar^F), 55.7 (s, CH_2), 40.2 (s, $SOMe_2$), 37.1 (s, NCH_3).

HR ESI-MS (180 °C, 4 kV) positive ion: 522.1155 ([*M* – $OSMe_2$]$^+$, calcd 522.1160) *m/z*.

Anal. Calcd for $C_{61}H_{43}BF_{24}N_5ORhS$ (1463.79 g mol^{-1}): C 50.05, H 2.96, N 4.78; found C, 49.86; H, 2.91; N, 4.70.

7. Preparation of [Rh(CNC-Me)(Ph)Cl(OSMe$_2$)][BAr$^F_4$] (4)

A solution of **1** (150 mg, 0.114 mmol) in chlorobenzene (6 mL) was heated at 50 °C for 8 h. The product was precipitated with excess hexane (*ca.* 10 mL), isolated by filtration, washed with hexane and dried in vacuo. Yield: 120 mg (74%).

^1H NMR (600 MHz, CD_2Cl_2): δ 7.85 (t, $^3J_{HH}$ = 7.8, 1H, py), 7.71–7.74 (m, 8H, Ar^F), 7.56 (br, 4H, Ar^F), 7.52 (d, $^3J_{HH}$ = 7.8, 1H, py), 7.28 (d, $^3J_{HH}$ = 7.8, 1H, py), 7.26 (d, $^3J_{HH}$ = 1.9, 1H, NCH), 7.18 (d, $^3J_{HH}$ = 7.2, 1H, Ph), 7.05 (d, $^3J_{HH}$ = 1.8, 1H, NCH), 6.99 (d, $^3J_{HH}$ = 1.8, 1H, NCH), 6.97 (d, $^3J_{HH}$ = 1.9, 1H, NCH), 6.79–6.86 (m, 2H, Ph), 6.45–6.49 (m, 1H, Ph), 6.44 (d, $^3J_{HH}$ = 15.4, 1H, CH_2), 5.27 (d, $^3J_{HH}$ = 7.6, 1H, Ph), 5.11 (d, $^3J_{HH}$ = 15.0, 1H, CH_2), 4.57 (d, $^3J_{HH}$ = 15.8, 1H, CH_2), 4.39 (s, 3H, NCH_3), 4.13 (d, $^3J_{HH}$ = 15.8, 1H, CH_2), 3.32 (s, 3H, NCH_3), 2.51 (s, 6H, $OSMe_2$).

$^{13}C\{^1H\}$ NMR (151 MHz, CD_2Cl_2): δ 174.6 (d, $^1J_{RhC}$ = 39, NCN), 174.0 (d, $^1J_{RhC}$ = 37, NCN), 162.3 (q, $^1J_{CB}$ = 50, Ar^F), 158.9 (s, py), 157.3 (s, py), 142.7 (d, $^1J_{RhC}$ = 32, Ph), 140.8 (s, Ph), 140.4 (s, py), 137.3 (s, Ph), 135.4 (s, Ar^F), 129.4 (qq, $^2J_{FC}$ = 32, $^3J_{CB}$ = 3, Ar^F), 127.6 (s, 2 × Ph), 127.0 (s, py), 126.3 (s, py), 125.2 (q, $^1J_{FC}$ = 272, Ar^F), 125.0 (s, NCH), 124.3 (s, NCH), 123.6 (s, Ph), 121.4 (s, NCH), 121.0 (s, NCH), 118.0 (sept, $^3J_{FC}$ = 4, Ar^F), 56.1 (s, CH_2), 55.6 (s, CH_2), 39.2 (s, $OSMe_2$), 38.9 (s, NCH_3), 38.0 (s, NCH_3).

HR ESI-MS (180 °C, 4 kV) positive ion: 482.0606 ([*M* – $OSMe_2$]$^+$, calcd 482.0613) *m/z*.

Anal. Calcd for $C_{55}H_{40}BClF_{24}N_5ORhS$ (1424.15 g mol^{-1}): C, 46.39; H, 2.83; N, 4.92; found C, 46.48; H, 2.68; N, 4.92.

8. Crystallographic details

Data were collected on a Rigaku Oxford Diffraction SuperNova AtlasS2 CCD diffractometer using graphite monochromated Mo K_α (λ = 0.71073 Å) or CuK_α (λ = 1.54184 Å) radiation and an Oxford Cryosystems N-HeliX low temperature device [150(2) K]. Data were collected and reduced using CrysAlisPro and refined using SHELXL,[27] through the Olex2 interface.[28]

Deposition Numbers 2022453 ([{Rh(PNP-*i*Pr)}$_2$(μ_2-η^2:η^2-COD)][BAr$^F_4$]$_2$), 2022454 (**2**), 2022455 (**3**), 2022456 (**4**) contain the supplementary crystallographic data for this paper. These data are provided free of charge by the joint Cambridge Crystallographic Data Centre and Fachinformationszentrum Karlsruhe Access Structures service www.ccdc.cam.ac.uk/structures.

9. Computational methods

All electronic structure calculations presented in this paper were carried out using the Gaussian 09 (Revision E.01)[29] program suite at the DFT level of theory. Geometries of all compounds were fully optimized without imposing symmetry constraints (C_1 symmetry), employing the Minnesota M06–L local meta-generalized gradient approximation (meta-GGA) functional.[30] The Stuttgart-Dresden (SDD)[31] relativistic effective core potential in combination with the associated basis sets were used to describe the Rh centre, augmented with an additional f-type polarisation function (ζ = 1.350).[32] The 6-31G(d,p) basis sets[33] developed by Pople and coworkers were used on all lighter atoms (C, Cl, N, and H). Optimized stationary points were characterized by analysis of their analytical second derivatives, with minima having only positive eigenvalues and transition states having exactly one imaginary eigenvalue. In order to identify the minima linked by each transition state, subsequent geometry optimizations were performed in both forward and reverse direction of the displacement vector of the transition state coordinate. The frequency calculations also provided thermal and entropic corrections to the total energy in gas phase at T = 298.15 K and p = 1 atm within the rigid-rotor/harmonic oscillator (RRHO) approximation. Dispersion effects were accounted for by applying Grimme's van der Waals correction (D3 parameterization[34]) during geometry optimizations of all stationary points. Effects due to the presence of a solvent were treated implicitly with a polarisable dielectric model, using the IEFPCM formalism in conjunction with Truhlar's SMD model.[35] In the absence of defined parameters for DFB solvent, default SMD parameters were selected for fluorobenzene and the relative permittivity adjusted to that of DFB (ε = 13.4).[36] All Gibbs energies are reported in kcal mol^{-1}. All structures were visualized using the Chemcraft tool.[37]

Conflicts of interest

There are no conflicts to declare.

Supporting information

- Additional computational details (PDF) and optimised geometries (XYZ)
- Primary NMR data (MNOVA)
- Accession Codes: CCDC 2022453–2022456 contain the supplementary crystallographic data for this paper.

Acknowledgments

We thank the European Research Council (ERC, grant agreement 637313; A. E. K., S. L., A. B. C.) and Royal Society (UF100592, UF150675, A. B. C.) for financial support. T. K. acknowledges the

DJEI/DES/SFI/HEA Irish Centre for High-End Computing (ICHEC) for the provision of computational facilities and support. High-resolution mass-spectrometry data were collected using instruments purchased through support from Advantage West Midlands and the European Regional Development Fund. Crystallographic data were collected using an instrument that received funding from the ERC under the European Union's Horizon 2020 research and innovation programme (grant agreement No 637313).

Keywords: Oxidative addition · Rhodium · Pincer ligands · Computational analysis · DFT calculations

[1] a) C. M. Storey, H. P. Cook, A. B. Chaplin in *Complexes of NHC-Based CEC Pincer Ligands* (Ed.: D. Morales-Morales), Elsevier, **2018**, vol. 1, pp. 173–189; b) R. E. Andrew, L. González-Sebastián, A. B. Chaplin, *Dalton Trans.* **2016**, *45*, 1299–1305.

[2] For selected recent examples see: a) T. Maulbetsch, E. Jürgens, D. Kunz, *Chem. Eur. J.* **2020**, *26*, 10634–10640; b) J. W. Nugent, M. García-Melchor, A. R. Fout, *Organometallics* **2020**, *39*, 2917–2927; c) W. Taniguchi, J.-I. Ito, M. Yamashita, *J. Organomet. Chem.* **2020**, *923*, 121436; d) Y. Arikawa, I. Tabata, Y. Miura, H. Tajiri, Y. Seto, S. Horiuchi, E. Sakuda, K. Umakoshi, *Chem. Eur. J.* **2020**, *26*, 5603–5606; e) S. Das, R. R. Rodrigues, R. W. Lamb, F. Qu, E. Reinheimer, C. M. Boudreaux, C. E. Webster, J. H. Delcamp, E. T. Papish, *Inorg. Chem.* **2019**, *58*, 8012–8020; f) K. Tokmic, B. J. Jackson, A. Salazar, T. J. Woods, A. R. Fout, *J. Am. Chem. Soc.* **2017**, *139*, 13554–13561; g) C. K. Ng, J. Wu, T. S. A. Hor, H.-K. Luo, *Chem. Commun.* **2016**, *52*, 11842–11845; h) K. Tokmic, A. R. Fout, *J. Am. Chem. Soc.* **2016**, *138*, 13700–13705; i) K. Tokmic, C. R. Markus, L. Zhu, A. R. Fout, *J. Am. Chem. Soc.* **2016**, *138*, 11907–11913; j) R. P. Yu, D. Hesk, N. Rivera, I. Pelczer, P. J. Chirik, *Nature* **2016**, *529*, 195–199.

[3] J. F. Hartwig, *Organotransition Metal Chemistry: From Bonding to Catalysis*; University Science Books, **2010**, vol. 1.

[4] a) R. E. Andrew, C. M. Storey, A. B. Chaplin, *Dalton Trans.* **2016**, *45*, 8937–8944; b) R. E. Andrew, D. W. Ferdani, C. A. Ohlin, A. B. Chaplin, *Organometallics* **2015**, *34*, 913–917; c) R. E. Andrew, A. B. Chaplin, *Inorg. Chem.* **2015**, *54*, 312–322; d) B. Wucher, M. Moser, S. A. Schumacher, F. Rominger, D. Kunz, *Angew. Chem. Int. Ed.* **2009**, *48*, 4417–4421; *Angew. Chem.* **2009**, *121*, 4481; e) M. Moser, B. Wucher, D. Kunz, F. Rominger, *Organometallics* **2007**, *26*, 1024–1030; f) J. M. Wilson, G. J. Sunley, H. Adams, A. Haynes, *J. Organomet. Chem.* **2005**, *690*, 6089–6095.

[5] a) C. M. Storey, M. R. Gyton, R. E. Andrew, A. B. Chaplin, *Chem Eur. J.* **2020**, *in the press*, DOI: https://doi.org/10.1002/chem.202002962; b) M. R. Gyton, A. E. Kynman, B. Leforestier, A. Gallo, J. R. Lewandowski, A. B. Chaplin, *Dalton Trans.* **2020**, *49*, 5791–5793; c) M. R. Gyton, B. Leforestier, A. B. Chaplin, *Organometallics* **2018**, *37*, 3963–3971; d) J. A. Wright, A. A. Danopoulos, W. B. Motherwell, R. J. Carroll, S. Ellwood, J. Saßmannshausen, *Eur. J. Inorg. Chem.* **2006**, *2006*, 4857–4865.

[6] G. Kleinhans, G. Guisado-Barrios, D. C. Liles, G. Bertrand, D. I. Bezuidenhout, *Chem. Commun.* **2016**, *52*, 3504–3507.

[7] a) Y. Tian, E. Jürgens, K. Mill, R. Jordan, T. Maulbetsch, D. Kunz, *ChemCatChem* **2019**, *11*, 4028–4035; b) Y. Tian, E. Jürgens, D. Kunz, *Chem. Commun.* **2018**, *54*, 11340–11343.

[8] C. M. Storey, M. R. Gyton, R. E. Andrew, A. B. Chaplin, *Angew. Chem. Int. Ed.* **2018**, *57*, 12003–12006; *Angew. Chem.* **2018**, *130*, 12179.

[9] M. Storey, A. Kalpokas, M. R. Gyton, T. Krämer, A. B. Chaplin, *Chem. Sci.* **2020**, *11*, 2051–2057.

[10] a) A. B. Chaplin, R. Tonner, A. S. Weller, *Organometallics* **2010**, *29*, 2710–2714; b) D. D. Wick, W. D. Jones, *Inorg. Chim. Acta* **2009**, *362*, 4416–4421; c) C. N. Iverson, W. D. Jones, *Organometallics* **2001**, *20*, 5745–5750; d) C. Perthuisot, W. D. Jones, *J. Am. Chem. Soc.* **1994**, *116*, 3647–3648.

[11] a) A. König, C. Fischer, E. Alberico, C. Selle, H.-J. Drexler, W. Baumann, D. Heller, *Eur. J. Inorg. Chem.* **2017**, *2017*, 2040–2047; b) Y. Jiao, W. W. Brennessel, W. D. Jones, *Organometallics* **2015**, *34*, 1552–1566; c) Y. Y. Qian, M. H. Lee, W. Yang, K. S. Chan, *J. Organomet. Chem.* **2015**, *791*, 82–89; d) T. M. Douglas, A. B. Chaplin, A. S. Weller, *Organometallics* **2008**, *27*, 2918–2921; e) V. V. Grushin, W. J. Marshall, *J. Am. Chem. Soc.* **2004**, *126*, 3068–3069; f) S. Willems, P. Budzelaar, N. Moonen, R. de Gelder, J. Smits, A. Gal, *Chem. Eur. J.* **2002**, *8*, 1310–1320.

[12] a) S. G. Curto, M. A. Esteruelas, M. Oliván, E. Oñate, A. Vélez, *Organometallics* **2017**, *36*, 114–128; b) S. D. Timpa, C. J. Pell, O. V. Ozerov, *J. Am. Chem. Soc.* **2014**, *136*, 14772–14779; c) M. Puri, S. Gatard, D. A. Smith, O. V. Ozerov, *Organometallics* **2011**, *30*, 2472–2482; d) J.-I. Ito, T. Miyakawa, H. Nishiyama, *Organometallics* **2008**, *27*, 3312–3315l; e) S. Gatard, C. Guo, B. M. Foxman, O. V. Ozerov, *Organometallics* **2007**, *26*, 6066–6075; f) S. Gatard, R. Çelenligil-Çetin, C. Guo, B. M. Foxman, O. V. Ozerov, *J. Am. Chem. Soc.* **2006**, *128*, 2808–2809.

[13] G. L. Parker, S. Lau, B. Leforestier, A. B. Chaplin, *Eur. J. Inorg. Chem.* **2019**, *2019*, 3791–3798.

[14] This routine complex was readily prepared using a method developed in our laboratories: M. R. Gyton, T. M. Hood, A. B. Chaplin, *Dalton Trans.* **2019**, *48*, 2877–2880. Full details are provided in the experimental section.

[15] The tetrafluroborate salt has been previously isolated: D. J. Nielsen, K. J. Cavell, B. W. Skelton, A. H. White, *Inorg. Chim. Acta* **2002**, *327*, 116–125.

[16] R. Dorta, H. Rozenberg, L. J. W. Shimon, D. Milstein, *Chem. Eur. J.* **2003**, *9*, 5237–5249.

[17] S. D. Pike, M. R. Crimmin, A. B. Chaplin, *Chem. Commun.* **2017**, *53*, 3615–3633.

[18] T. M. Hood, B. Leforestier, M. R. Gyton, A. B. Chaplin, *Inorg. Chem.* **2019**, *58*, 7593–7601.

[19] D. A. Laviska, C. Guan, T. J. Emge, M. Wilklow-Marnell, W. W. Brennessel, W. Jones, W. D. Jones, K. Krogh-Jespersen, A. S. Goldman, *Dalton Trans.* **2014**, *43*, 16354–16365.

[20] a) L. Souillart, N. Cramer, *Chem. Rev.* **2015**, *115*, 9410–9464; b) C.-H. Jun, *Chem. Soc. Rev.* **2004**, *33*, 610–618; c) B. Rybtchinski, D. Milstein, *Angew. Chem. Int. Ed.* **1999**, *38*, 870–883; *Angew. Chem.* **1999**, *111*, 918.

[21] Adoption of a *fac*-coordination mode does, however, require substantial structural reorganisation following insertion into the C–Cl bond to afford **4**. In addition to the "direct" pathway depicted in Figure 4, a higher energy variant was also identified with a calculated barrier of $\Delta G^{\ddagger}$ = 34.3 kcal mol^{-1} from **1**. Full details are provided in the ESI.

[22] H. Wu, M. B. Hall, *J. Phys. Chem. A* **2009**, *113*, 11706–11712.

[23] S. Gründemann, M. Albrecht, J. A. Loch, J. W. Faller, R. H. Crabtree, *Organometallics* **2001**, *20*, 5485–5488.

[24] a) A. J. Martínez-Martínez, A. S. Weller, *Dalton Trans.* **2019**, *48*, 3551–3554; b) W. E. Buschmann, J. S. Miller, K. Bowman-James, C. N. Miller, *Inorg. Synth.* **2002**, *33*, 83–91.

[25] E. Neumann, A. Pfaltz, *Organometallics* **2005**, *24*, 2008–2011.

[26] W. P. Leung, Q. W. Y. Ip, S. Y. Wong, T. C. W. Mak, *Organometallics* **2003**, *22*, 4604–4609.

[27] G. M. Sheldrick, *Acta Crystallogr., Sect. C* **2015**, *71*, 3–8.

[28] O. V. Dolomanov, L. J. Bourhis, R. J. Gildea, J. A. K. Howard, H. Puschmann, *J. Appl. Crystallogr.* **2009**, *42*, 339–341.

[29] M. J. Frisch, G. W. Trucks, H. B. Schlegel, G. E. Scuseria, M. A. Robb, J. R. Cheeseman, G. Scalmani, V. Barone, B. Mennucci, G. A. Petersson, H. Nakatsuji, M. Caricato, X. Li, H. P. Hratchian, A. F. Izmaylov, J. Bloino, G. Zheng, J. L. Sonnenberg, M. Hada, M. Ehara, K. Toyota, R. Fukuda, J. Hasegawa, M. Ishida, T. Nakajima, Y. Honda, O. Kitao, H. Nakai, T. Vreven, J. A. Montgomery Jr., J. E. Peralta, F. Ogliaro, M. Bearpark, J. J. Heyd, E. Brothers, K. N. Kudin, V. N. Staroverov, R. Kobayashi, J. Normand, K. Raghavachari, A. Rendell, J. C. Burant, S. S. Iyengar, J. Tomasi, M. Cossi, N. Rega, J. M. Millam, M. Klene, J. E. Knox, J. B. Cross, V. Bakken, C. Adamo, J. Jaramillo, R. Gomperts, R. E. Stratmann, O. Yazyev, A. J. Austin, R. Cammi, C. Pomelli, J. W. Ochterski, R. L. Martin, K. Morokuma, V. G. Zakrzewski, G. A. Voth, P. Salvador, J. J. Dannenberg, S. Dapprich, A. D. Daniels, Ö. Farkas, J. B. Foresman, J. V. Ortiz, J. Cioslowski, D. J. Fox, *Gaussian 09, Revision E.01*, Gaussian, Inc., Wallingford CT, **2013**.

[30] a) Y. Zhao, D. G. Truhlar, *J. Chem. Phys.* **2006**, *125*, 194101; b) Y. Zhao, D. G. Truhlar, *Acc. Chem. Res.* **2008**, *41*, 157–167.

[31] D. Andrae, U. Häußermann, M. Dolg, H. Stoll, H. Preuß, *Theor. Chim. Acta* **1990**, *77*, 123–141.

[32] A. W. Ehlers, M. Böhme, S. Dapprich, A. Gobbi, A. Höllwarth, V. Jonas, K. F. Köhler, R. Stegmann, A. Veldkamp, G. Frenking, *Chem. Phys. Lett.* **1993**, *208*, 111–114.
[33] a) W. J. Hehre, R. Ditchfield, J. A. Pople, *J. Chem. Phys.* **1972**, *56*, 2257–2261; b) P. C. Harihara, J. A. Pople, *Theor. Chim. Acta* **1973**, *28*, 213–222.
[34] S. Grimme, J. Antony, S. Ehrlich, H. Krieg, *J. Chem. Phys.* **2010**, *132*, 154104.
[35] A. V. Marenich, C. J. Cramer, D. G. Truhlar, *J. Phys. Chem. B* **2009**, *113*, 6378–6396.
[36] T. R. O'Toole, J. N. Younathan, B. P. Sullivan, T. J. Meyer, *Inorg. Chem.* **1989**, *28*, 3923–3926.
[37] G. A. Zhurko, D. A. Zhurko, G. A. Andrienko, *Chemcraft*, Version 1.8 (Build 536).

Received: August 16, 2020